Cell J
Cell Journal(Yakhteh)
Homepage: https://www.celljournal.org/
Original Article
Vol 25, No 8, August 2023, Pages: 524-535

Umbilical Cord Blood-Derived Monocytes as A Reliable Source of Functional Macrophages for Biomedical Research

Shukoofeh Torabi, Ph.D.[1, 2], Morteza Zarrabi, M.D., Ph.D.[1, 3], Nikoo Hossein-Khannazer, Ph.D.[4], Majid Lotfinia, Ph.D.[5], Masoumeh Nouri, Ph.D.[3], Roberto Gramignoli, Ph.D.[6, 7*], Moustapha Hassan, Ph.D.[8], Massoud Vosough, M.D., Ph.D.[1, 8*]

1. Department of Regenerative Medicine, Cell Science Research Center, Royan Institute for Stem Cell Biology and Technology, ACECR, Tehran, Iran
2. Department of Applied Cell Sciences, Faculty of Basic Sciences and Advanced Medical Technologies, Royan Institute, ACECR, Tehran, Iran
3. R & D Department, Royan Stem Cell Technology Co, Tehran, Iran
4. Gastroenterology and Liver Diseases Research Center, Research Institute for Gastroenterology and Liver Diseases, Shahid Beheshti University of Medical Sciences, Tehran, Iran
5. Physiology Research Center, Kashan University of Medical Sciences, Kashan, Iran
6. Department of Laboratory Medicine, Division of Pathology, Karolinska Institute, Stockholm, Sweden
7. Department of Pathology and Cancer Diagnostic, Karolinska University Hospital, 141 83 Stockholm, Sweden
8. Experimental Cancer Medicine, Institution for Laboratory Medicine, and Karolinska University Hospital, Karolinska Institute, Stockholm, Sweden

Abstract

Objective: Macrophages are multifunctional immune cells widely used in immunological research. While autologous macrophages have been widely used in several biomedical applications, allogeneic macrophages have also demonstrated similar or even superior therapeutic potential. The umbilical cord blood (UCB) is a well-described source of abundant allogenic monocytes and macrophages that is easy to collect and can be processed without invasive methods. Current monocyte isolation procedures frequently result in heterogenous cell products, with limited yields, activated cells, and high cost. This study outlines a simple isolation method that results in high yields and pure monocytes with the potential to differentiate into functional macrophages.

Materials and Methods: In the experimental study, we describe a simple and efficient protocol to isolate high-purity monocytes. After collection of human UCB samples, we used a gradient-based procedure composed of three consecutive gradient steps: i. Hydroxyethyl starch-based erythrocytes sedimentation, followed by ii. Mononuclear cells (MNCs) isolation by Ficoll-Hypaque gradient, and iii. Separation of monocytes from lymphocytes by a slight hyperosmolar Percoll gradient (0.573 g/ml). Then the differentiation potential of isolated monocytes to pro- and anti-inflammatory macrophages were evaluated in the presence of granulocyte colony-stimulating factor (GM-CSF) and macrophage CSF (M-CSF), respectively. The macrophages were functionally characterized as well.

Results: A high yield of monocytes after isolation (25 to 50 million) with a high purity (>95%) could be obtained from every 100-150 ml UCB. Isolated monocytes were defined based on their phenotype and surface markers expression pattern. Moreover, they possess the ability to differentiate into pro- or anti-inflammatory macrophages with specific phenotypes, gene/surface protein markers, cytokine secretion patterns, T-cell interactions, and phagocytosis activity.

Conclusion: Here we describe a simple and reproducible procedure for isolation of pure monocytes from UCB, which could be utilized to provide functional macrophages as a reliable and feasible source of allogenic macrophages for biomedical research.

Keywords: Macrophage Polarization, Monocytes, Umbilical Cord Blood

Citation: **Torabi Sh, Zarrabi M, Hossein-Khannazer N, Lotfinia M, Nouri M, Gramignoli R, Hassan M, Vosough M. Umbilical cord blood-derived monocytes as a reliable source of functional macrophages for biomedical research. Cell J. 2023; 25(8): 524-535. doi: 10.22074/CELLJ.2023.1990203.1238**
This open-access article has been published under the terms of the Creative Commons Attribution Non-Commercial 3.0 (CC BY-NC 3.0).

Introduction

Human umbilical cord blood (UCB) represents a rich and complex population of stem/progenitor cells and diverse immunogenic and tolerogenic subsets of the innate and adaptive immune cells. For several decades, UCB represented an inexhaustible source of quality cells for off-the-shelf products in translational medicine (1). Several studies have profiled the role of $CD34^+$/$CD133^+$/$VEGFR2^+$ endothelial progenitor cells in promoting tissue regeneration and healing, but fewer reports

Received: 21/February/2023, Revised: 15/May/2023, Accepted: 21/May/2023
***Corresponding Addresses: Department of Laboratory Medicine, Division of Pathology, Karolinska Institutet, Stockholm, Sweden**
P.O.Box: 16635-148, Department of Regenerative Medicine, Cell Science Research Center, Royan Institute for Stem Cell Biology and Technology, ACECR, Tehran, Iran
Emails: roberto.gramignoli@Ki.se, masvos@royaninstitute.org

Royan Institute
Cell Journal (Yakhteh)

have highlighted the critical role of $CD14^+$ monocytes derived from UCBs which represent a valuable source of progenitor cells capable of differentiating into dendritic cells (DCs) or macrophages (2, 3). Monocytes/macrophages are the primary mononuclear phagocytic cells that are subdivided in two major subtypes: M1 pro-inflammatory macrophages, involved in antigen presentation, promoting inflammation, and pathogen phagocytosis; M2 anti-inflammatory macrophages tied to immune tolerance, tissue remodeling, and resolution of inflammation and wound healing (4, 5).

In addition to application of autologous monocytes in order to modulate inflammation and autoimmune responses (6-8), allogeneic monocytes/macrophages have also been evaluated for their therapeutic potential in tissue repair and regeneration induction. An allogeneic cell transplant of programmable cells of monocytic origin (PCMO) resulted in improved angiogenesis and tissue repair in a hind limb ischemia model by regulating muscle stem cell proliferation, circulating mononuclear cell (MNC) recruitment, and switching inflammatory monocytes to anti-inflammatory macrophages (9). Moreover, as compared to autologous monocyte transplantation, in a rabbit model of femoral neck ischemia, allogenic $CD14^+$ monocyte transplantation significantly enhanced arteriogenesis through the paracrine effect of secreted growth factors and cytokines and facilitated monocyte recruitment (10).

Several studies have also demonstrated that UCB-derived monocytes are a reliable source of allogeneic cells and have similar or even superior regenerative capacities to adult tissues, in terms of tissue repair and wound healing capacity, angiogenesis induction, and anti-inflammatory responses (11-13). Compared to the adult peripheral blood (PB) monocytes, UCB-derived monocytes effectively phagocyte the Amyloid-β (Aβ) plaques, and mediate cognitive and motor functions in a transgenic model of Alzheimer's disease (14).

Moreover, UCB-derived monocyte cell therapy products (DUOC-01) have shown a great potential in promoting brain remyelination in cuprizone-treated mice. Preclinical characterization of these cells showed that DUOC-01 cells are highly active, motile, well tolerated and proliferating cells with similar morphological and functional properties of brain macrophage and microglia that persist in the brain and spinal cord for at least 56 days after injection. All these data suggest DUOC-01 as a cell-based treatment option for patients with demyelinating conditions such as multiple sclerosis or spinal cord injury (15, 16).

Several techniques have been reported to isolate monocytes from whole blood and each one has its own advantages and disadvantages, in particular in relation to the purity and yield of non-activated cells. Using positive or negative immune selection is a widely described method for generating high-purity monocytes. In large-scale production, such protocols are often constrained by expensive reagents. Moreover, immune selection frequently results in activated monocytes (13, 17, 18). However, the vast majority of protocols use density gradient centrifugation, an inexpensive, simple, reproducible, and easy method. The most popular method currently used to isolate monocytes from MNCs is the Ficoll-Hypaque gradient centrifugation followed by a round of adherent cells selection. Such an approach is frequently accompanied by high lymphocytic contamination, time-consuming manipulations, poor cell recovery, and partial activation of monocytes (18). The centrifugal elutriation approach also requires large volumes of blood samples, qualified lab technicians, and expensive equipment (19, 20). With basic laboratory equipment and personnel, we can efficiently isolate monocytes from human UCB using a three-step gradient-based procedure. The procedure described here is a simple and cost-effective method to provide a remarkable yield and purity of functional UCB-derived monocytes for biomedical research.

Materials and Methods

Chemicals and reagents

SedimSure 6% hydroxyethyl starch (HES, WAK-Chemie Medical GmbH, 870009), Ficoll-paque ™ PLUS 1.077 (CYTIVA GE, 17144002), Percoll Plus® (Sigma-Aldrich, P1644), Iscove's Modified Dulbecco's Medium (IMDM, Gibco™, 12200-069), Human Albumin 20% Solution (CSL Behring, 4597/349), fetal bovine serum (FBS, Gibco™, 16000044), GlutaMAX™ Supplement (Gibco™, 35050-061), Penicillin-Streptomycin (Gibco™, 15070-063), MEM Non-Essential Amino Acids Solution (Gibco™, 11140050), Human Platelet Lysate (hPL, Royan Institute, Iran), CliniMACS® PBS/EDTA Buffer (Miltenyi Biotec, 130-070-525), Ethylenediaminetetraacetic Acid Powder (EDTA, Sigma-Aldrich, E9884), phosphate-buffered saline (PBS) tablets (Sigma-Aldrich, 003002), human recombinant macrophage colony-stimulating factor (M-CSF, Thermo Scientific™, RP-8643), human recombinant granulocyte-macrophage CSF (GM-CSF, R&D system, 215-GM-010), CellTrace™ CFSE Cell Proliferation Kit (Thermo Scientific™, D8417), Phytohemagglutinin-M (PHA-M, Thermo Scientific™, 10576015), Luria-Bertani Medium (Sigma-Aldrich, L7658), Ampicillin (Sigma-Aldrich, A9518), 4′,6-Diamidino-2-phenylindole Dihydrochloride (DAPI, Sigma-Aldrich, D8417).

Preparation of solutions

Ficoll-Paque solution

Twelve ml of Ficoll-paque was mixed thoroughly with 500 µl PBS (1X) by vortex to form a homogenous solution.

PBS/EDTA/Plasma

One ml of autologous plasma was added to 25 ml of PBS/EDTA (1 mM).

Stock solution of Percoll (SIP)

Eighteen ml of Percoll (density 1.130 ± 0.005 g/ml) was

diluted with 2 ml PBS (10X) to make of density 1.124 g/ml, pH=8.2.

Hyper-osmotic Percoll solution

Ten ml of SIP was vigorously mixed with 9.5 ml PBS /EDTA/ Plasma.

Iso-osmotic Percoll solution

Eight ml SIP was vigorously mixed with 11 ml PBS /EDTA/ Plasma.

Density gradient isolation procedure

During this experimental study, gradient isolation is performed sequentially: i. Erythrocytes are separated using 6% HES solution, ii. MNCs are isolated using Ficoll gradient, and iii. Monocytes are separated from lymphocytes by hyperosmolar Percoll gradient.

Separation of erythrocytes

UCB samples were obtained from the placentae of healthy infants immediately after delivery. Iggnformed consent was obtained according to the Ethics Committee of Royan Institute guidelines (IR.ACECR.ROYAN.REC.1399.056). The blood was collected in a bag containing 35 ml of citrate phosphate dextrose adenine (CPDA-1) solution and transported to the laboratory for further processing. To reduce the risk of granulocyte contamination the blood samples were processed for MNCs isolation within 3 hours after collection. In one-fifth volume of the blood samples, HES 6% was added to the (CPDA) whole blood resulting in a 1.2% HES in the CPDA/whole blood/HES solution. For every 100 ml of blood, 20 ml of 6% HES was added. The solution was mixed by shaking the bag for 10 minutes and allowed to stand for about 90 minutes for the separation of blood components by gravity. After the erythrocyte sedimentation, the upper plasma layer (containing leukocytes and platelets) was aliquoted out into separate tubes and immediately centrifuged at 2800 × *g* for 10 minutes.

Isolation of mononuclear cells

After centrifugation, the supernatant plasma was collected in a 50 ml tube, leaving approximately 6 ml of plasma above the pelleted cells. The pelleted cells were resuspended in the plasma remaining in the tube, and 6 ml of 1 mM PBS/EDTA was added to the solution. The Ficoll-Paque mixture (3 ml) was added to the bottom of four 15 ml centrifuge tubes. The Ficoll-Paque-containing tubes were held horizontally at an angle of 10-15 degrees and the blood mixture (6 ml) was carefully layered above the Ficoll-Paque mixture. The tubes were centrifuged at 950 × *g* for 30 minutes at room temperature (RT) with no brake. In the next step, the collected plasma was centrifuged at 2.800 × *g* for 10 minutes in order to sediment platelets and cell debris. The purified plasma was stored in separate tubes for further steps.

Monocyte purification

The dense white mononuclear band at the interface between the Ficoll-Paque and the plasma-medium layers from two tubes were collected into a new 50 ml tube. The collected cells were washed twice with 45 ml of PBS/EDTA (1 mM, 450 × *g* for 10 minutes at RT). Then, the supernatant was discarded and pelleted cells were resuspended in 8 ml IMDM supplemented with 1000 U/ml penicillin/streptomycin, 2 mM GlutaMAX™, 0.1 mM nonessential amino acids and 5% autologous plasma. First, 4 ml of RT hyperosmotic Percoll solution was added to four 15 ml tubes. Then, 4 ml of iso-osmotic Percoll solution was smoothly layered on top. Afterwards, 2 ml of MNC suspension was slowly layered above the Percoll solution and centrifuged at 800 × *g* for 30 minutes at RT, with no brake. The white band above the iso-osmotic Percoll containing platelets, debris, and dead cells was carefully discarded, and the monocytes within the band at the junction of iso-osmotic and hyper-osmotic Percoll were collected in a new 50 ml tube. The cell suspension was diluted with 2.5 ml of PBS/EDTA/plasma and finally 1mM PBS/EDTA was added to the top. The tube was centrifuged at 350 × *g* for 10 minutes at RT. The supernatant was discarded, and cells were resuspended in 1 ml IMDM supplemented with 1000 U/ml penicillin/streptomycin, 2 mM GlutaMAX™, 0.1 mM non-essential amino acids, and 0.5% hPL for monocyte attachment. To isolate monocytes, 8×10^6 to 10×10^6 of the enriched monocytic population were plated in a non-treated 60 mm petri dish (Oosafe®, OOPW-ST06) at 2×10^6 to $2\text{-}5\times10^6$/ml in 4 ml IMDM supplemented with 1000 U/ml penicillin/streptomycin, 2 mM GlutaMAX™ , 0.1 mM nonessential amino acids and 0.5% hPL, and were allowed to adhere in a 5% CO_2 incubator at 37°C for 1 hour. Non-adherent cells were removed, adherent cells were thoroughly washed twice with 1 mM PBS/EDTA and the medium was replaced with IMDM containing1000 U/ml penicillin/ streptomycin, 2 mM GlutaMAX™ , 0.1 mM nonessential amino acids and 5% hPL.

Monocytes culture and macrophage differentiation

Monocytes were cultured in 6-well culture plates in RPMI, DMEM/F12, or IMDM mediums supplemented with either 0.5-10% FBS, human serum (HS), or hPL. Cell adhesion and morphological features of cells were analyzed by inverted light microscopy after a culture period of 7 days. Cells cultured in IMDM supplemented with 5% hPL showed a better differentiation capacity compared to other mediums. For later sets of experiments, purified monocytes were cultured in 6-well non-tissue culture plates (Corning Costar®, 3736) at a concentration of 1×10^6 cells/ml in the conventional maturation media (IMDM supplemented with 1000 U/ml penicillin/streptomycin, 2 mM GlutaMAX™, 0.1 mM nonessential amino acids, and 5% hPL) or a maturation media containing 100 ng/ml GM-CSF or 100 ng/ml M-CSF for 7 days to generate naïve, pre-M1 or pre-M2 macrophages, respectively. Approximately every two to three days, the media were changed.

Flow cytometry analysis

To determine cell heterogeneity, 1×10^5 monocytes (in 50 µl PBS containing 1% FBS) were stained for the expression of cell surface markers: CD45-FITC (BD Pharmingen™, USA, 345808), CD14-PE (Biolegend, USA, 367104), CD3-PerCP (Biolegend, USA, 344813), CD19-PE (EXBIO Praha, Czechia, 1P-305), CD16-FITC (Szabo-Scandic, Austria, IMS16F2). After 30 minutes of incubation at 4°C with antibody, PBS was used twice to wash the cells. Macrophage subsets were detached with 5 mM PBS/EDTA (40 minutes, 4°C), washed with PBS, and stained with CD14-PE (Biolegend, USA, 367104), CD206-FITC (Biolegend, USA, 321104), CD163-PE (Biolegend, USA, 333606), CD80-PE (BD Pharmingen™, USA, 557227), CD86-PE (BD Pharmingen™, USA, 555658), and CD83 (BioRad, USA, MCA1582F) as described above. Live cells were gated using forward scatter vs. side scatter plots to exclude apoptotic or dead cell debris 7-amino-actinomycin D (7-AAD, Biolegend, USA, 420403). Data were acquired using (BD FACSCalibur Flow Cytometer: 4-Color) and data analysis was performed using the FlowJo 7.6.exe (Tree Star Inc, Ashland, OR).

RNA extraction and quantitative real-time polymerase chain reaction

RNA from the stimulated macrophages was extracted using NucleoSpin RNA, Mini kit (MACHEREY-NAGELGmbH, Germany) according to the manufacturer's recommendation and was reverse transcribed to cDNA using RevertAid H Minus First Strand cDNA Synthesis Kit (Thermo Scientific™, K1632) for 5 min (65°C), 5 minutes (25°C) 60 minutes (42°C) and followed by a 5 minutes (70°C) incubation. The expression of interleukin 10 (*IL-10*), transforming growth factor beta (*TGF-β*), DC-specific intercellular adhesion molecule-3-grabbing non-integrin (*DC-SIGN*), Resistin-like molecule alpha1 (*Fizz1*), *CD163,* mannose receptor C-type 1 (*MRC1*), *CD80,* Interleukin1 beta (*IL-1β*), tumor necrosis factor alpha (*TNF-α*), and interleukin 6 (*IL-6*) were analyzed by quantitative polymerase chain reaction (PCR) using SYBR® Premix Ex Taq™ II (TaKaRa, RR820) on the ABI StepOnePlus Real-Time PCR system (40 cycles of 95°C for 15 seconds, 60°C for 15 seconds, and 72°C for 15 seconds). The level of gene expression was calculated using the $2^{-\Delta\Delta CT}$ method using glyceraldehyde-3-phosphate dehydrogenase (GAPDH) as the endogenous control. The PCR primer sequences are listed in Table S1 (See Supplementary Online Information at www.celljournal.org).

Soluble cytokines measurment

Human TNF-α, TGF-β, IL-6, and IL-10 were measured in the conditioned media of differentiated macrophages by ELISA (R&D Systems™ ELISA Kit, D1000B, DTA00D, D6050, and E0134Hu) according to the manufacturer's instructions.

Phagocytosis assay

To evaluate the phagocytosis capacity of the stimulated macrophages, upon maturation on day 7, the medium was replaced with IMDM without penicillin/streptomycin and hPL, overnight. For bacterial inoculation into macrophages, enhanced green fluorescent protein (EGFP) expressing *E.coli* were cultured in LB broth containing 100 µg/ml ampicillin (16 hours, 37°C, Shaker incubator 125 rpm). After centrifugation at 4000 rpm for 10 minutes, the bacterial pellet was resuspended and washed with 14 ml of ice-cold PBS for 10 min (4000 rpm, 4°C). Then, EGFP-positive bacteria were opsonized with human AB^+ serum as a source of complement components for 2 hours at 37°C and 80 rpm. *E.coli* suspensions were centrifuged (10 minutes, 4000 rpm), and the bacterial pellet was resuspended with pre-warmed IMDM without penicillin/streptomycin and counted to control the multiplicity of infection (MOI), approximately at 20. Stimulated macrophages were then incubated with opsonized bacteria for 120 minutes at 37°C. Phagocytosis was stopped by placing the cell culture plates on ice to kill all remaining extracellular bacteria, macrophages were incubated with gentamicin (200 µg/ml) for 15 minutes at 37°C. The phagocytic capacity of the cells was evaluated by inverted fluorescence microscopy or flow cytometric analysis. For fluorescence microscopy, macrophages were washed twice with ice-cold PBS and fixed with 4% paraformaldehyde for 10 minutes at RT. After the washing steps, the cells were stained with 4′,6-diamidino-2-phenylindole (DAPI) and examined with a fluorescence microscope (Olympus IX71). For flow cytometric analysis, inoculated macrophages were washed (PBS 1X), trypsinized for 20 minutes, and resuspended in ice-cold PBS (BD FACSCalibur™).

T-Cell proliferation assay

To evaluate the proliferation rate of allogenic T-cells in the presence of differentiated Pre-M1 or Pre-M2 macrophages, PB mononuclear cells (PBMCs) were isolated from healthy blood donors and cell adhesion was performed to eliminate the monocytic population. For T-cell staining, the cell suspension was collected and centrifuged at 350 × *g* for 10 minutes, and the pellet containing T cells was resuspended in 1 ml PBS (1X) and incubated in the dark with 5 µM carboxyfluorescein succinimidyl ester (CFSE) for 5 minutes. After washing steps (3 times), T-cells were seeded in 96-well plates (SPL, 34296) containing RPMI medium supplemented with 10% FBS in the presence of 5 µg/ml of phytohaemagglutinin (PHA) as the cell proliferation inducer. Then, Pre-M1 and Pre-M2 macrophages were harvested and added to the wells using a ratio of 1:2 macrophages to T-cells. On day 5, T-cells were stained with anti-CD3 (PE) (Biolegend, 300408) and the proliferation rate was analyzed by flow cytometry.

Statistical analysis

All experiments were performed in monocytes isolated from at least three different healthy donors. Statistical comparison between groups was performed by one-way

ANOVA followed by Tukey's post hoc test (*; P<0.05, **; P<0.01, ***; P<0.001) using GraphPad Prism 9 (version 9.0.0, GraphPad Software, Inc. USA). Results are presented as mean ± SD (n=3-6).

Results

The three-step gradient-based isolation technique resulted in pure monocytes

The three-step gradient-based isolation was tested and performed on at least 6 human UCB sample(s) (Fig.1A). The percentages of $CD14^+$ monocytes were measured in different human UCB samples by cytofluorimetric analysis. In agreement with previous studies (21, 22), our results showed higher frequency (mean percentage 7.5%) of UCB-derived monocytes in comparison to adult PB samples (Fig.S1, See Supplementary Online Information at www.celljournal.org). In each isolation step, to evaluate the viability and purity of cells, the viability of isolated cells has been measured by trypan blue and the monocyte-to-lymphocyte ratio was determined by flow cytometric analysis. We observed cell viability >95% in the cell populations obtained from all donors. The flow cytometric analysis, based on the forward scatter (FSC) vs. side scatter (SSC) pseudocolor dot plots and Giemsa staining of the cells, revealed a significant increase in the monocytic population in each step from erythrocyte sedimentation to monocyte adherence (Fig.1B, C). Immunophenotyping analysis indicated the mean percentage of $CD14^+$ monocytes in the $CD45^+$ leukocytes population (11% in MNCs), rising to 46 and 95% after Percoll gradient and attachment to cell culture plate, respectively (Fig.2A, B). Furthermore, higher percentages of classical ($CD14^+$/$CD16^-$) monocytes (94%), and intermediate ($CD14^+$/$CD16^+$) monocytes (4%) were found among the adherent cells (Fig.2A). The frequency of $CD3^+$ T-cells and $CD19^+$ B-cells exhibited a decreasing trend with median range (58 to 3% in $CD3^+$ T-cells/19% to less than 1% in $CD19^+$ B-cells) from Ficoll-Paque gradient to adherent culture (Fig.2C, D). Finally, the average monocyte yield was 9.5% according to the initial MNC's numbers, as determined by cell counting.

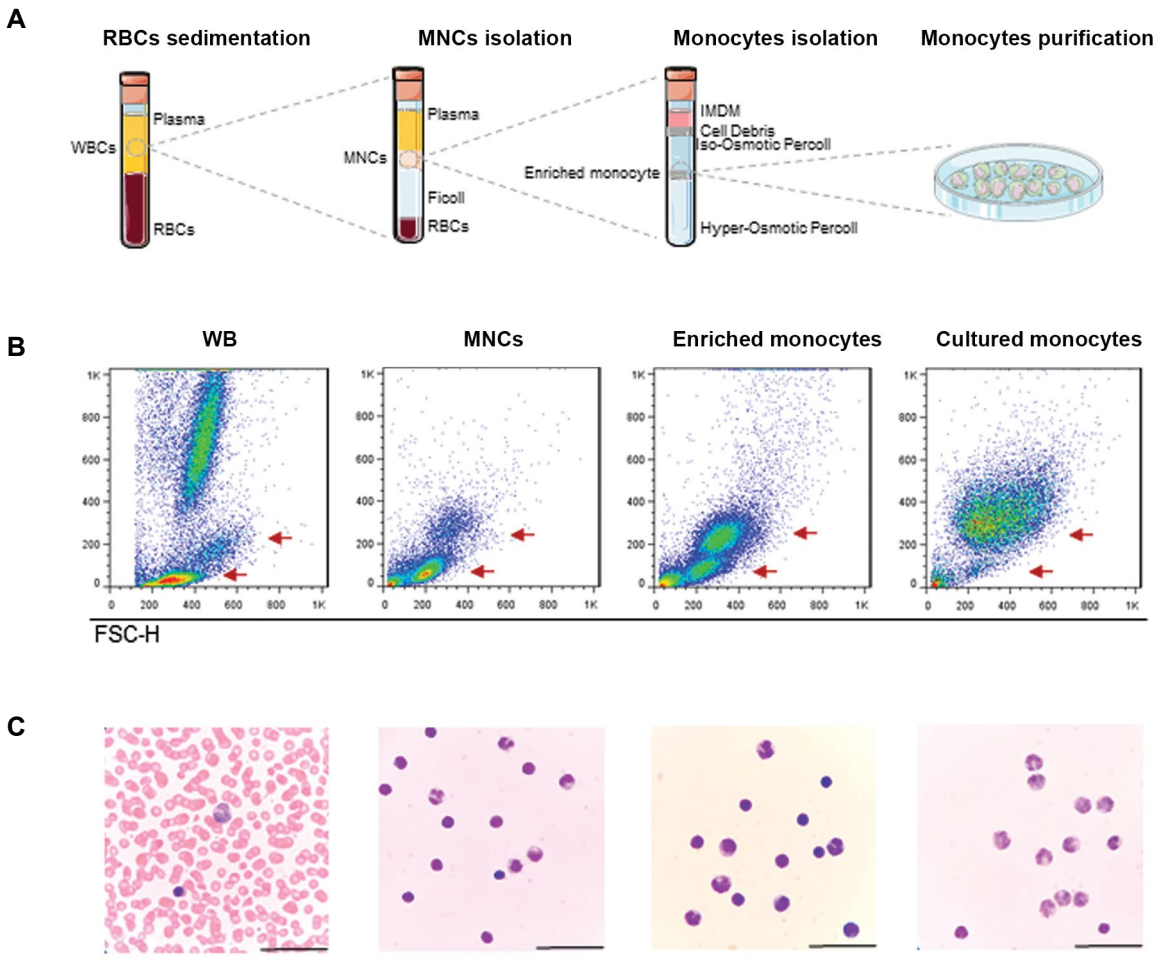

Fig.1: The process of UCB-derived monocytes isolation. **A.** UCB-derived monocytes isolation started with erythrocytes sedimentation using HES, MNCs isolation by Ficoll-Hypaque gradient, monocyte isolation by hyperosmolar Percoll gradient and monocyte purification after plastic adhesion. **B.** Forward scatter versus side scatter and arrows denote the change in lymphocyte and monocyte populations in every isolation step. **C.** Representative images of lymphocytes and monocytes in WB, MNCs, Enriched monocyte and cultured monocyte populations taken by Olympus CX31 microscope (Giemsa staining, 40× magnification, scale bar: 50 µm). UCB; Umbilical cord blood, HES; Hydroxyethyl starch, MNCs; Mononuclear cells, WB; Whole blood, and RBCs; Red blood cells.

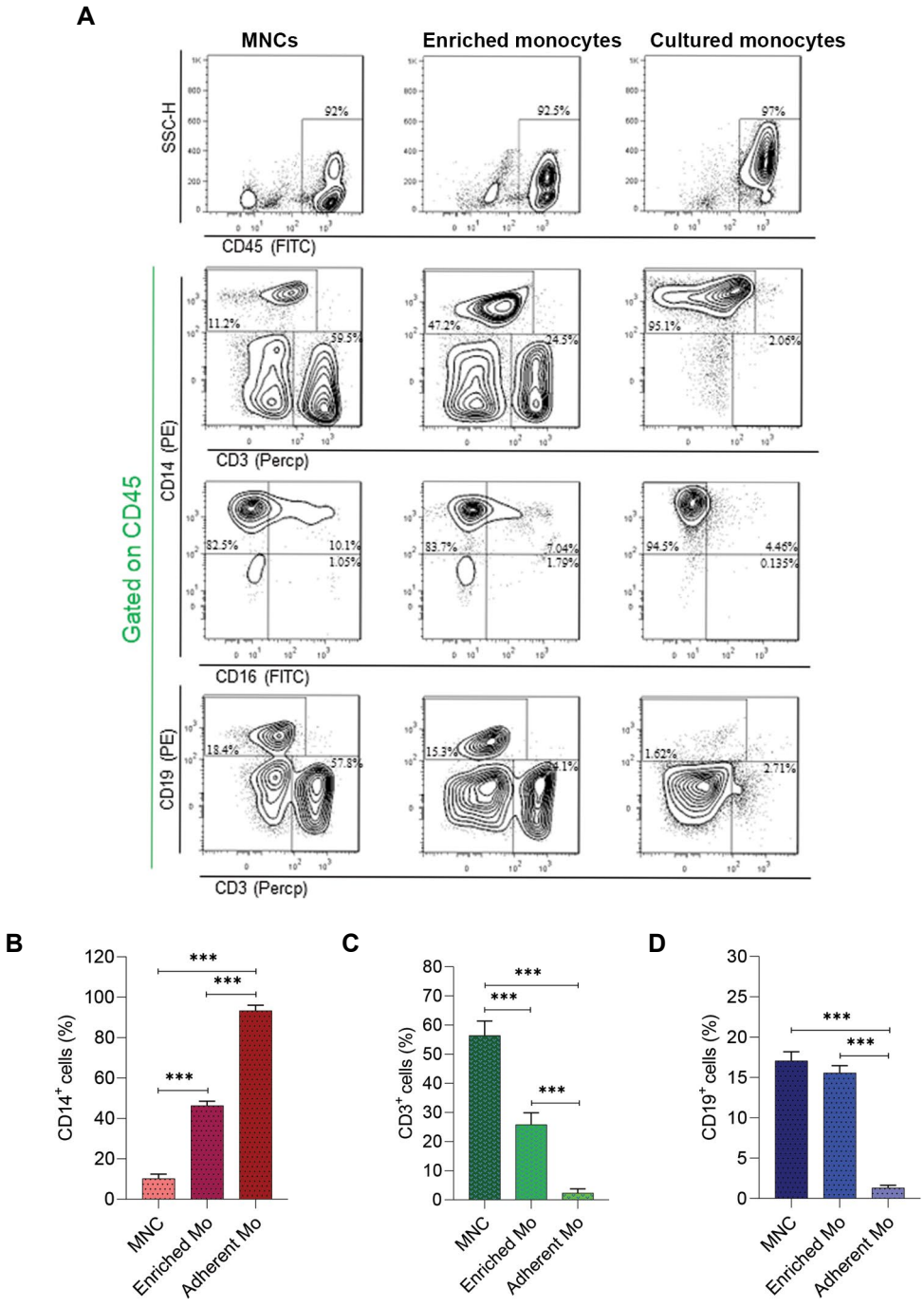

Fig.2: Purity and phenotype of isolated UCB-derived monocytes. Monocytes were isolated from UCB by a three-step gradient-based procedure, MNCs isolation by Ficoll-Hypaque gradient, Mo isolation by hyperosmolar Percoll gradient and Mo purification after plastic adhesion. After isolation, the purity and distribution of isolated monocyte subpopulations were analyzed by flow cytometry. **A.** Monocyte purity: The top panel shows the percentages of $CD45^+$ leukocytes after every isolation step. The middle panels show $CD3^+$lymphocytes/$CD14^+$monocytes gated on $CD45^+$ cells and monocyte subpopulations were sub-divided based on CD14 and CD16 expression as classical ($CD14^{high}CD16^{neg/low}$), intermediate ($CD14^{high}CD16^{high}$) and non-classical ($CD14^{low}CD16^{high}$) (within the live/ single monocyte gate). The bottom panel shows gating $CD3^+$T-cells and $CD19^+$B-Cells (within the live/$CD45^+$gate) in every isolation step. The expression levels of **B.** CD14, **C.** CD3 and **D.** CD19 positive cells after every step isolation were evaluated. Column bars are representative mean ± SD of data obtained from six healthy donors. Statistically significant differences were determined by one-way ANOVA followed by Tukey's post hoc test, n=6. ***; P<0.001, UCB; Umbilical cord blood, MNCs; Mononuclear cells, and Mo; Monocyte.

Morphology and gene expression profile were different in monocyte-derived pre-M1 and pre-M2 macrophages

We initially compared three different media supplemented with different concentrations of FBS, hPL, and HS, to evaluate the effect of different media and sera on the cellular phenotype, adhesion, and viability. During the monocyte isolation procedure, we found that IMDM medium supplemented with 0.5% hPL allowed superior attachment in monocytes, and macrophages cultivated in a similar medium supplemented with 5% hPL displayed the morphological characteristics typical of mature macrophages, as cultured in DMEM/F12 or RPMI formulations (Fig.S2, See Supplementary Online Information at www.celljournal.org). Once media and sera were selected, UCB-derived monocytes were differentiated into pre-M1 and pre-M2 macrophages by

exposure to GM-CSF or M-CSF for 7 days, respectively. Giemsa staining and flow cytometric analysis proved their differentiation by elucidating changes in the size and shape of cells. The naïve macrophages (untreated cells) displayed a mixture of round and spindle-shaped cells (Fig.3A). The majority of pre-M1 macrophages showed a round and "fried egg" morphology (Fig.3B). While pre-M2 cells predominantly exhibited a spindle-like morphology (Fig.3C). The mRNA expression pattern of M1- and M2-like macrophages (differentiated cells) revealed higher expression levels of *TNF-α, IL-1β, IL-6, CD80,* and mannose-binding lectin receptor *MRC1 (CD206)* for pre-M1 macrophages, in comparison to naïve and pre-M2 cells. However, pre-M2 macrophages exhibited a higher expression of *DC-SIGN* (*CD209*), *Fizz1*, scavenger receptor *CD163*, *TGF-β* and *IL-10* compared to naïve and pre-M1 macrophages (Fig.3D). Overall, these results support that UCB-derived monocytes can effectively differentiate into M1- and M2-like macrophages in the presence of GM-CSF or M-CSF, respectively.

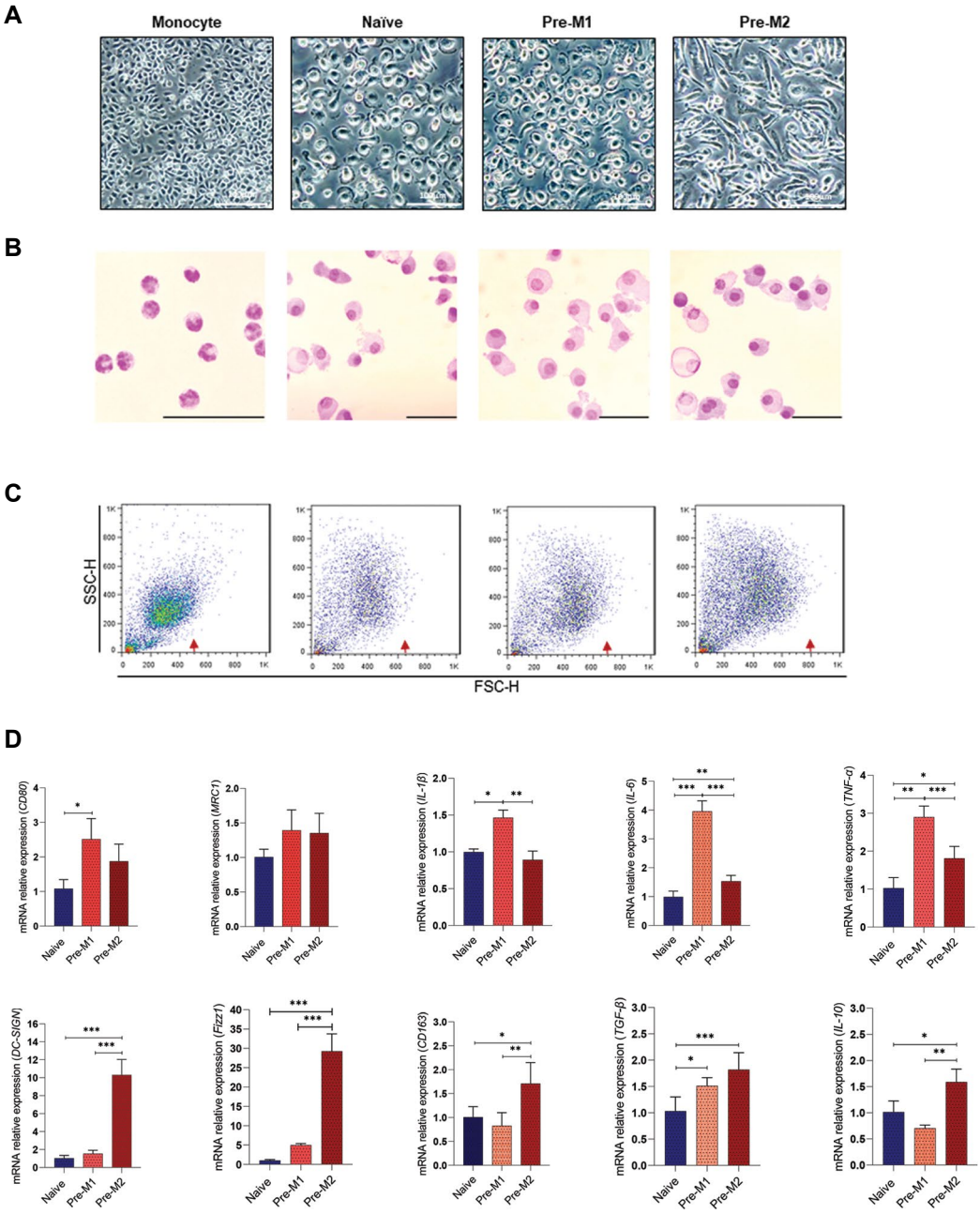

Fig.3: Monocyte-derived macrophages characterization. Monocytes isolated from the UCB were cultured and differentiated into macrophages using complete IMDM media, GM-CSF, and M-CSF for 7 days to produce naive, pre-M1 and pre-M2 macrophages, respectively. **A.** Morphology of differentiated macrophages was assessed by light microscopy (scale bar: 100 µm), **B.** Giemsa staining (scale bar: 50 µm) and **C.** Flow cytometry according to forward scatter versus side scatter characteristics. **D.** mRNA expression changes in polarized macrophages were determined by quantitative RT-PCR. Column bars represent the mean ± SD of three independent experiments with macrophages from three different healthy donors. Statistically significant differences were determined by one-way ANOVA followed by Tukey's post hoc test. *; P<0.05, **; P<0.01, ***; P<0.001, UCB; Umbilical cord blood, GM-CSF; Granulocyte-macrophage colony stimulating factor, M-CSF; Macrophage colony stimulating factor, and RT-PCR; Reverse transcription polymerase chain reaction.

Pre-M1 and pre-M2 macrophages displayed different surface markers

We analyzed common surface markers which are associated with M1 and M2 phenotypes. FACS analysis experiments showed that pre-M2 macrophages expressed higher levels of CD14, CD163, and CD86. In contrast, the expression of CD80 and CD206 was higher in pre-M1 macrophages compared to naïve and pre-M2 macrophages. Moreover, all macrophages were negative for the expression of CD83, a specific surface marker of mature DCs which confirmed that isolated monocytes do not differentiate into DCs (Fig.4A). Therefore, in agreement with gene expression patterns, differentiated cells, phenotypically indicated the expected macrophage lineage markers as they were negative for expression of DC-specific markers, besides the higher expression level of M1- and M2-like specific markers.

Functional characterization confirmed successful differentiation of macrophage subsets

The phagocytic activity of differentiated macrophages was assessed after incubation with a GFP-labeled bacteria (*E.coli*) for 2 hours, followed by flow cytometric analysis and fluorescent microscopy. Representative images and cytofluorimetric analysis show a higher percentage of phagocytosed bacteria in pre-M1 and pre-M2 macrophages comparable to those of naïve macrophages (Fig.5A, B). Furthermore, to evaluate the impact of macrophage co-culture on activation status and proliferative activity of lymphocytes, pre-M1 and pre-M2 macrophages were co-cultured for 5 days with CFSE labeled PBMCs. The proliferation rate of $CD3^+$ T-cells was evaluated by cytofluorimetric analysis. As shown in Figure 5C, D, we measured a significant inhibition in the proliferation of $CD3^+$ cells in the presence of pre-M2 macrophages. Furthermore, measuring the expression of pro- and anti-inflammatory cytokines in the supernatant of differentiated macrophages resulted in high expression of TNF-α and IL-6 in pre-M1, with significant upregulation in anti-inflammatory cytokines IL-10 and TGF-β in the supernatant of pre-M2 macrophages (Fig.5E). Such a finding is in line with our results indicating that GM-CSF and M-CSF can generate functional and activated macrophages with typical phenotype, gene and surface marker expression, and cytokine secretion pattern from UCB-derived monocytes.

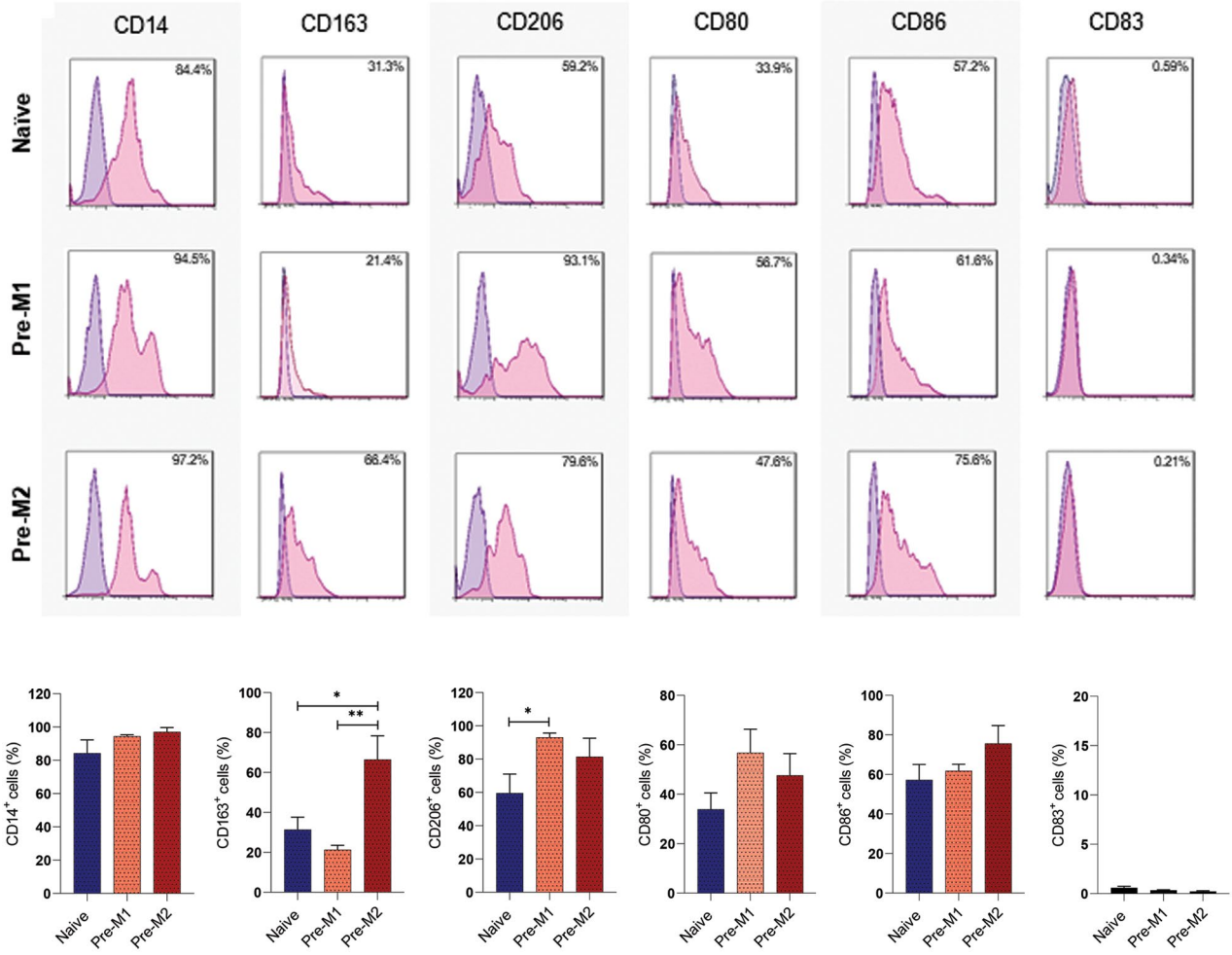

Fig.4: Surface marker expression pattern of differentiated macrophages. Naïve, pre-M1, and pre-M2 macrophages were generated in 7 days as described above. Data are expressed as percentages of positive and negative cell surface markers as mean ± SD of three independent experiments with macrophages from three different healthy donors. Statistically significant differences were determined by one-way ANOVA followed by Tukey's post hoc test. *; P<0.05, and **; P< 0.01.

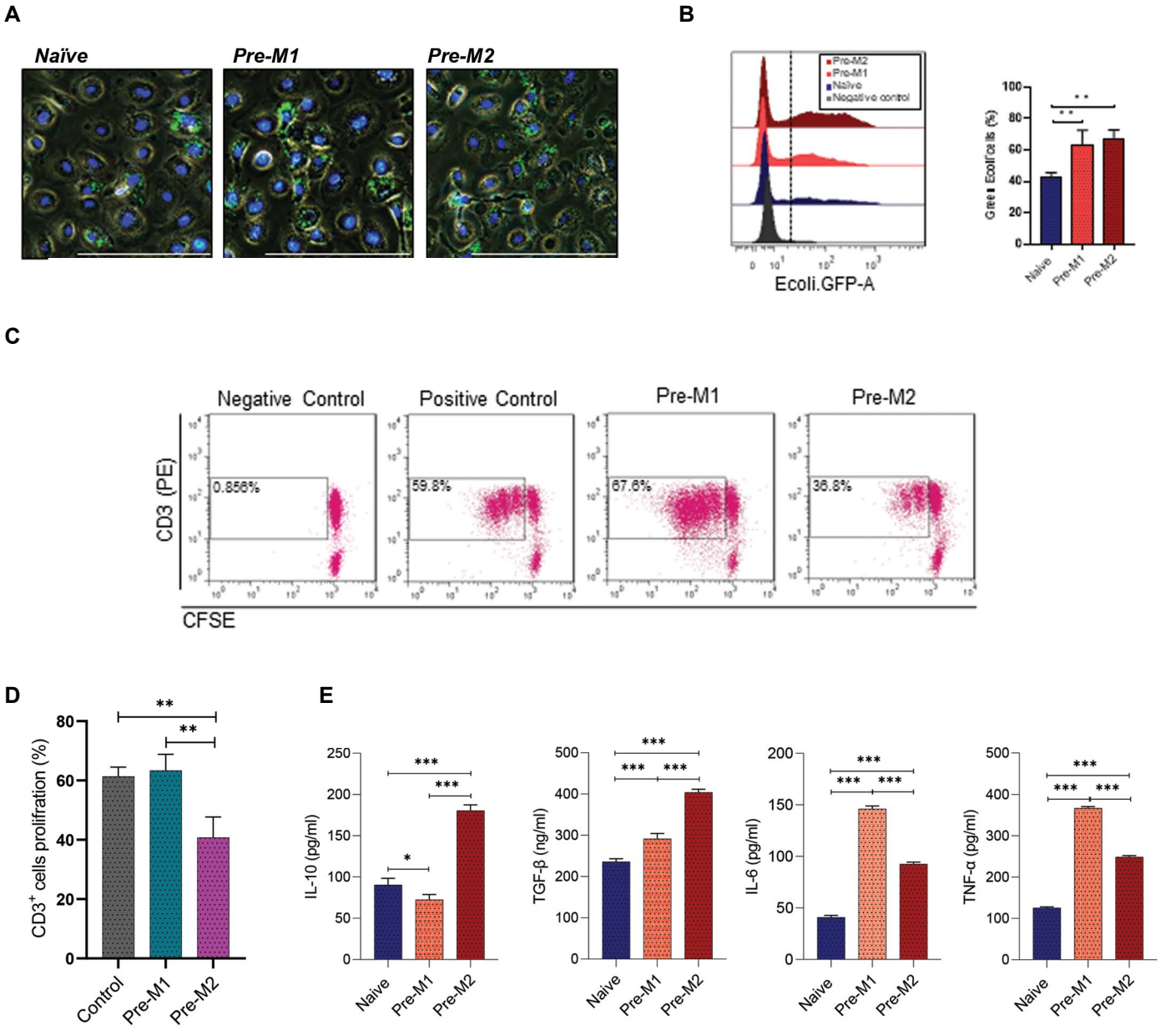

Fig.5: Functional assessment of differentiated macrophages. UCB-derived monocytes were polarazied into naïve, pre-M1, and pre-M2 in the presence of complete IMDM media, GM-CSF, or M-CSF for 7 days, respectively. **A.** The phagocytic activity of macrophages was analyzed after incubation with GFP-labeled *E.coli* for 2 hours at 37°C by fluorescent microscopy (scale bar: 100 µm) and **B.** Quantification of phagocytic activity of cells using flow cytometric analysis. **C.** The proliferation rates of CFSE-labeled $CD3^+$ lymphocytes in the presence of pre-M1 or pre-M2 macrophages (lymphocyte to macrophage ratio of 2:1) were analyzed after 5 days by flow cytometry. **D.** The mean ± SD of the percentages of $CD3^+$ proliferating cells. **E.** ELISA was used to measure the levels of cytokines in polarized macrophage culture supernatants. Column bars represent the mean ± SD of three independent experiments with macrophages from three different healthy donors. Statistically significant differences were determined by one-way ANOVA followed by Tukey's post hoc test. **; P<0.01, ***; P<0.001, UCB; Umbilical cord blood, GM-CSF; Granulocyte-macrophage colony stimulating factor, M-CSF; Macrophage colony stimulating factor, and CFSE; Carboxyfluorescein succinimidyl ester.

Discussion

Human UCB have been investigated for the safety of their use in a variety of medical conditions e.g. autoimmune diseases, damaged bone and cartilage repair, neurologic, cardiovascular, hematopoitic malignancies and hepatic disorders (22-26). High purity and quality of hematopoietic stem and progenitor cells, immunological immaturity of the cells, as well as higher telomerase activity and *in vitro* proliferation potential are essential for the successful therapeutic application of human UCB cells (27). The monocytes are a highly plastic subset of blood progenitor cells that play a key role in innate immunity, and they can either differentiate into DCs or macrophages. The UCB is an excellent source of monocytes and macrophages that can be obtained easily, and without using invasive procedures. However, very little research has been conducted to evaluate the potential benefits of application of UCB-derived monocytes in regenerative medicine as an allogeneic "off-the-shelf" cell product.

Our study developed a three-step procedure for efficiently isolating a large number of pure monocytes. Next, we assessed whether these isolated cells were able

to differentiate into functional macrophages. During the isolation protocol, several alternative approaches have been developed to provide a reproducible and solid MNCs population. Despite the efficacy of performing sedimentation in order to remove erythrocytes, we experienced different levels of remaining erythrocytes in the MNC's population (section above the Ficoll-Paque surface) which usually results in lymphocyte trapping. Another challenge was granulocyte contamination which resulted in low purity and heterogenicity in isolated MNCs. To overcome such challenges, three different strategies were implemented. i. The first strategy was reducing the Ficoll-Paque density, similar to the Normann protocol (2). The decreased Ficoll-Paque density was found to impair erythrocyte aggregation and prevent granulocyte precipitation. ii. The second approach to improve the overall outcome was found in reducing the time (<4 hours) between the blood collection and cell isolation. iii. In the third strategy diluted blood was gradually overlaid on a specific angle over the Ficoll-Paque layer to avoid disturbing the separation between the medium and blood (interface). Monocytes are usually isolated by adherence after Ficoll-Hypaque purification of MNCs. According to previous results, monocyte purity in this approach was approximately 70% under optimal conditions, and because of high lymphocyte contamination, the number of adherent monocytes was significantly lower than in comparison to immune selection techniques. We also observed 62% purity of $CD14^+$ cells after culturing MNCs (data not shown). Hence, we developed a three step gradient protocol that in contrast to the high number of lymphocytes in UCB compared to PB (28), yielded a higher number ($2.5\text{-}5\times10^7$ cells/100-150 ml UCB) and purity (>95%) of monocytes, comparable or even superior to the adherence method after Ficoll-Hypaque gradient (18, 29). After monocyte culture and macrophage differentiation, the attached cells should be detached for phenotyping and functional characterization. Since the macrophages are tightly adherent cells, we tested and validated different enzymatic solutions (Trypsin, Accutase, TrypLE) or non-enzymatic approaches (different concentrations of PBS/EDTA), at different temperatures (37°C and 4°C) or incubation times (10 to 40 minutes). In agreement with previous studies (30, 31), we found that enzymatic approaches resulted in higher cell yield and viability. However, such an invasive method cleaves several surface markers, including CD163 and CD206. Alternatively, prolonged exposure (40 minutes) to 5 mM PBS/EDTA (at 4°C) was found instrumental to preserve the phenotypic and functional characterization of macrophages. Nevertheless, cell viability decreased up to 70%. The flow cytometric analysis demonstrated high yield and purity of isolated monocytes, which confirmed the validity and robustness of the protocol. We examined the ability of UCB-derived $CD14^+$ monocytes to produce functional pro- and anti-inflammatory macrophages in response to stimulatory cytokines. After induction of isolated monocytes with GM-CSF and MCSF, the polarized pre-M1 and pre-M2 macrophages showed significant differences in mRNA expression patterns, surface and secreted markers, similar to findings of studies conducted on PB-derived macrophages (31-33). Gene expression pattern and secretion of pro-inflammatory cytokines such as TNF-α, and IL-6, as well as upregulation of genes and surface markers of co-stimulatory molecules, CD80, and CD206 in pre-M1 macrophages proved the impact of GM-CSF in the induction of pro-inflammatory phenotype of macrophages. A previous study also observed, UCB derived macrophages showed similar expression of cell surface markers CD40, CD80, HLA-DR, CD86 and CD206 compared to the adult macrophages when stimulated with LPS or Mycobacterium tuberculosis (Mtb) (34). Nevertheless, the high expression of anti-inflammatory cytokines (TGF-β, IL-10), up-regulation of scavenger receptors (CD163, CD209), and induction of Fizz1 as the indicator of JAK1/STAT6 signaling pathway activation in pre-M2 macrophages showed that M-CSF treatment induced notable changes in monocytic genes and protein expression after differentiation to anti-inflammatory macrophages.

Studies have found similarities between PB-derived macrophages and UCB-derived macrophages with respect to phagocytosis, degradation activity, and ROS production (35, 36). Our results are in agreement with other studies and demonstrated that UCB-derived macrophages were able to perform phagocytosis of *E. coli,* similar to macrophages derived from PB (37, 38). A further observation was that both pre-M1 and pre-M2 macrophages were able to phagocytose bacteria more efficiently than naive cells. This may be related to enhanced expression of CD206 (in pre-M1) as well as CD209 and CD163 (in pre-M2) macrophages (35). Finally, the upregulation of IL-10 and TGF-β, the main modulators of T-cells resulted in the inhibition of $CD3^+$ cell proliferation in the presence of pre-M2 macrophages. On the contrary, the high proliferation rate measured in the presence of pre-M1 macrophages and enhanced secretion of pro-inflammatory cytokines promoted the activation and proliferation of $CD3^+$ cells. All in all, our findings indicated that UCB could be used as a reliable and feasible source of allogenic functional macrophages that may serve as an alternative source of autologous macrophages for basic and applied biomedical research.

Conclusion

While still considered a biological waste product, UCB may offer valuable support for clinical and diagnostic purposes in future biomedical research. Particularly, the isolated cells from UCB can provide a great promise in future research and therapies. The higher proportion of naïve and progenitor cells in UCB compared to the PB has increased the possibility of their potential application in non-hematopoietic diseases and as an alternative cell source for regenerative medicine, tissue engineering, and immune modulation practices. Our present results also showed that UCB could be a reliable and alternative source of monocytes in translational studies. The protocol described here provides a simple, cost-effective, and reproducible procedure for the isolation of UCB-derived

monocytes in small/large volumes. Monocytes derived from this protocol had high yield, purity, and viability. These cells were successfully polarized to pro- and anti-inflammatory macrophages and harbor a significant potential as a consistent and reliable source of antigen-presenting cell source for regenerative medicine approaches.

Acknowledgments

We would like to express our sincere gratitude to our colleagues at Royan Institute, and at Karolinska Institute. This study was funded by grants from Bahar Tashkhis Teb Co (BT-9906), Royan Institute (R1399- 99000082), and Royan Stem Cell Technology (RST- 99000082) to MV, and a grant from Åke Wiberg Stiftelse (nr.M20-0192) to RG. There is no conflict of interest in this study.

Authors' Contributions

S.T.; Conceptualization, Methodology, Software Data Curation, and Writing original draft. M.Z., N.H.-K., M.L., MN.; Formal analysis, Review, Editing, and Validation. M.H., R.G.; Conceptualization, Review, Editing, and Supervision. M.V.; Conceptualization, Supervision, Project administration, Funding acquisition, Review, and Editing. All authors read and approved the final manuscript.

References

1. Allan DS. Using umbilical cord blood for regenerative therapy: proof or promise? Stem Cells. 2020; 38(5): 590-595.
2. Normann E, Lacaze-Masmonteil T, Winkler-Lowen B, Guilbert LJ. Isolation of non-activated monocytes from human umbilical cord blood. Am J Reprod Immunol. 2010; 63(1): 66-72.
3. Scott RA, Kiick KL, Akins RE. Substrate stiffness directs the phenotype and polarization state of cord blood derived macrophages. Acta Biomater. 2021; 122: 220-235.
4. Hamidzadeh K, Christensen SM, Dalby E, Chandrasekaran P, Mosser DM. Macrophages and the recovery from acute and chronic inflammation. Annu Rev Physiol. 2017; 79: 567-592.
5. Oishi Y, Manabe I. Macrophages in inflammation, repair and regeneration. Int Immunol. 2018; 30(11): 511-528.
6. Wilson HM, Stewart KN, Brown PA, Anegon I, Chettibi S, Rees AJ, et al. Bone-marrow-derived macrophages genetically modified to produce IL-10 reduce injury in experimental glomerulonephritis. Mol Ther. 2002; 6(6): 710-717.
7. Costa-Marques L, Arnold K, Pardon MC, Leovsky C, Swarbrick S, Fabian C, et al. Transplantation of bone marrow derived macrophages reduces markers of neuropathology in an APP/PS1 mouse model. Transl Neurodegener. 2019; 8: 33.
8. Podaru MN, Fields L, Kainuma S, Ichihara Y, Hussain M, Ito T, et al. Reparative macrophage transplantation for myocardial repair: a refinement of bone marrow mononuclear cell-based therapy. Basic Res Cardiol. 2019; 114(5): 34.
9. Berndt R, Hummitzsch L, Heß K, Albrecht M, Zitta K, Rusch R, et al. Allogeneic transplantation of programmable cells of monocytic origin (PCMO) improves angiogenesis and tissue recovery in critical limb ischemia (CLI): a translational approach. Stem Cell Res Ther. 2018; 9(1): 117.
10. Herold J, Pipp F, Fernandez B, Xing Z, Heil M, Tillmanns H, et al. Transplantation of monocytes: a novel strategy for in vivo augmentation of collateral vessel growth. Hum Gene Ther. 2004; 15(1): 1-12.
11. Namakula R, de Bree LCJ, A Tvedt TH, Netea MG, Cose S, Hanevik K. Monocytes from neonates and adults have a similar capacity to adapt their cytokine production after previous exposure to BCG and β-glucan. PLoS One. 2020; 15(2): e0229287.
12. Saha A, Patel S, Xu L, Scotland P, Schwartzman J, Filiano AJ, et al. Human umbilical cord blood monocytes, but not adult blood monocytes, rescue brain cells from hypoxic-ischemic injury: Mechanistic and therapeutic implications. PLoS One. 2019; 14(9): e0218906.
13. Sohlberg E, Saghafian-Hedengren S, Bremme K, Sverremark-Ekström E. Cord blood monocyte subsets are similar to adult and show potent peptidoglycan-stimulated cytokine responses. Immunology. 2011; 133(1): 41-50.
14. Darlington D, Li S, Hou H, Habib A, Tian J, Gao Y, et al. Human umbilical cord blood-derived monocytes improve cognitive deficits and reduce amyloid-β pathology in PSAPP mice. Cell Transplant. 2015; 24(11): 2237-2250.
15. Kurtzberg J, Buntz S, Gentry T, Noeldner P, Ozamiz A, Rusche B,et al. Preclinical characterization of DUOC-01, a cell therapy product derived from banked umbilical cord blood for use as an adjuvant to umbilical cord blood transplantation for treatment of inherited metabolic diseases. Cytotherapy. 2015; 17(6): 803-815.
16. Saha A, Buntz S, Scotland P, Xu L, Noeldner P, Patel S, et al. A cord blood monocyte-derived cell therapy product accelerates brain remyelination. JCI Insight. 2016; 1(13): e86667.
17. Fluks AJ. Three-step isolation of human blood monocytes using discontinuous density gradients of Percoll. J Immunol Methods. 1981; 41(2): 225-233.
18. Nielsen MC, Andersen MN, Møller HJ. Monocyte isolation techniques significantly impact the phenotype of both isolated monocytes and derived macrophages in vitro. Immunology. 2020; 159(1): 63-74.
19. de Almeida MC, Silva AC, Barral A, Barral Netto M. A simple method for human peripheral blood monocyte isolation. Mem Inst Oswaldo Cruz. 2000; 95(2): 221-223.
20. Meital LT, Coward AS, Windsor MT, Bailey TG, Kuballa A, Russell FD. A simple and effective method for the isolation and culture of human monocytes from small volumes of peripheral blood. J Immunol Methods. 2019; 472: 75-78.
21. Prabhu SB, Rathore DK, Nair D, Chaudhary A, Raza S, Kanodia P, et al. Comparison of human neonatal and adult blood leukocyte subset composition phenotypes. PLoS One. 2016; 11(9): e0162242.
22. Cunningham S, Hackstein H. Cord-blood-derived professional antigen-presenting cells: functions and applications in current and prospective cell therapies. Int J Mol Sci. 2021; 22(11): 5923.
23. de Haar C, Plantinga M, Blokland NJ, van Til NP, Flinsenberg TW, Van Tendeloo VF, et al. Generation of a cord blood-derived Wilms Tumor 1 dendritic cell vaccine for AML patients treated with allogeneic cord blood transplantation. Oncoimmunology. 2015; 4(11): e1023973.
24. McDonald CA, Penny TR, Paton MCB, Sutherland AE, Nekkanti L, Yawno T, et al. Effects of umbilical cord blood cells, and subtypes, to reduce neuroinflammation following perinatal hypoxic-ischemic brain injury. J Neuroinflammation. 2018; 15(1): 47.
25. Phuc PV, Ngoc VB, Lam DH, Tam NT, Viet PQ, Ngoc PK. Isolation of three important types of 26 cells from the same samples of banked umbilical cord blood. Cell Tissue Bank. 2012; 13(2): 341-351.
26. Rizk M, Aziz J, Shorr R, Allan DS. Cell-based therapy using umbilical cord blood for novel indications in regenerative therapy and immune modulation: an updated systematic scoping review of the literature. Biol Blood Marrow Transplant. 2017; 23(10): 1607-1613.
27. Riordan NH, Chan K, Marleau AM, Ichim TE. Cord blood in regenerative medicine: do we need immune suppression? J Transl Med. 2007; 5: 8.
28. Yun HD, Varma A, Hussain MJ, Nathan S, Brunstein C. Clinical relevance of immunobiology in umbilical cord blood transplantation. J Clin Med. 2019; 8(11): 1968.
29. Chometon TQ, Siqueira MDS, Sant Anna JC, Almeida MR, Gandini M, Martins de Almeida Nogueira AC, et al. A protocol for rapid monocyte isolation and generation of singular human monocyte-derived dendritic cells. PLoS One. 2020; 15(4): e0231132.
30. Feuerer N, Morschl J, Daum R, Weiss M, Hinderer S, Schenke-Layland K, et al. Macrophage retrieval from 3D biomaterials: a detailed comparison of common dissociation methods. J Immunol Regen Med. 2021; 11: 100035.
31. Chen S, So EC, Strome SE, Zhang X. Impact of detachment methods on M2 Macrophage phenotype and function. J Immunol Methods. 2015; 426: 56-61.
32. Lukic A, Larssen P, Fauland A, Samuelsson B, Wheelock CE, Gabrielsson S, et al. GM-CSF- and M-CSF-primed macrophages present similar resolving but distinct inflammatory lipid mediator signatures. FASEB J. 2017; 31(10): 4370-4381.

33. Bazzi S, El-Darzi E, McDowell T, Modjtahedi H, Mudan S, Achkar M, et al. Defining Genome-wide expression and phenotypic contextual cues in macrophages generated by granulocyte/macrophage colony-stimulating factor, macrophage colony-stimulating factor, and heat-killed mycobacteria. Front Immunol. 2017; 8: 1253.
34. Ó Maoldomhnaigh C, Cox DJ, Phelan JJ, Malone FD, Keane J, Basdeo SA. The warburg effect occurs rapidly in stimulated human adult but not umbilical cord blood derived macrophages. Front Immunol. 2021; 12: 657261.
35. Dreschers S, Ohl K, Schulte N, Tenbrock K, Orlikowsky TW. Impaired functional capacity of polarised neonatal macrophages. Sci Rep. 2020; 10(1): 624.
36. Gille Ch, Leiber A, Mundle I, Spring B, Abele H, Spellerberg B, et al. Phagocytosis and postphagocytic reaction of cord blood and adult blood monocyte after infection with green fluorescent protein-labeled Escherichia coli and group B Streptococci. Cytometry B Clin Cytom. 2009; 76(4): 271-284.
37. Lam RS, O'Brien-Simpson NM, Holden JA, Lenzo JC, Fong SB, Reynolds EC. Unprimed, M1 and M2 macrophages differentially interact with porphyromonas gingivalis. PLoS One. 2016; 11(7): e0158629.
38. Cao X, Yakala GK, van den Hil FE, Cochrane A, Mummery CL, Orlova VV. Differentiation and functional comparison of monocytes and macrophages from hiPSCs with peripheral blood derivatives. Stem Cell Reports. 2019; 12(6): 1282-1297.